Formation of transverse mode in axially symmetric lasers

V. G. Niziev[1,*] and D. Toebaert[2]

[1]Institute on Laser and Information Technologies, Russian Academy of Sciences, Shatura, Moscow Region, 140700, Russia

[2]ELAS NV, Slachthuisstraat 53-59, B-7700 Moeskroen, Belgium

*Corresponding author: niziev@yahoo.com

Received 7 October 2011; revised 21 November 2011; accepted 4 December 2011; posted 6 December 2011 (Doc. ID 156107); published 29 February 2012

The developed iteration algorithm for simulation of lasers with an open resonator was employed in the study of transverse mode formation. The simulations of an axially symmetrical resonator rely on an analytical description of radiation diffraction from a narrow ring. Reflection of an incident wave with a specified amplitude-phase distribution from the mirror is calculated by the Green-function method. The model also includes an active medium homogeneous along the resonator axis that is represented by the formula for saturating gain. The calculations were performed for two types of lasers: with on-axis and off-axis gain maximum. In the first type of laser one can obtain either a principal mode or "multimode" generation. The latter means quasi-stationary generation with regular or chaotic oscillations. In the second type of laser high order single-mode generation is possible. Experimental results obtained on a fast axial flow 4 kW CO_2 laser are also presented. They are in good agreement with the calculations.

OCIS code: 140.3410, 030.4070, 140.4780, 260.1960, 230.5750.

I. Introduction

The problem of optical resonator simulation has been considered repeatedly, both analytically and numerically [1–4], for empty resonators as well as for lasers with an active medium. In spite of this, the problem cannot be regarded as a finally solved one.

For example, there exists a broad class of high-power lasers featuring high gain in the active medium and a low-quality resonator. The beam quality in these lasers is expected to depend on the time of transverse mode formation in the resonator. If this time is long, there can be no hope for a quality close to the ideal beam. Another example is from the area of pulsed (or pulse-periodic) lasers. As the transverse structure of radiation starts to be formed in each of the pulses, the time of mode formation in the selected resonator should be compared with the laser pulse duration for the beam quality to be generally characterized. In present-day pulsed lasers, pulse duration can range from femtoseconds to milliseconds. Both examples are indicative of the cognitive and practical expediency of studying the process of transverse mode formation in laser resonators. Apart from this, there are many other interesting and important problems such as the physical nature of "multimode generation" and the conditions of multipass ray mode generation.

In [5] a new method of resonator simulation for axially symmetric field distributions was developed based on Fox and Li algorithm, and used in studying the dynamics of field distribution formation in empty resonators. It was shown that, depending on the resonator parameters, the process of mode formation proceeds according to different types of relaxation oscillations. The wave based resonator simulation reveals "paraxial resonances" predicted in [6] by the methods of ray optics.

1559-128X/12/070954-09$15.00/0

The present paper is a logical continuation of [5]. Now the process of transverse mode formation will be considered for a laser having some active medium. This work is aimed at the investigation of the specific features of transverse mode formation in lasers of different types.

2. Mathematical Model

In all the problems to be solved below we shall restrict ourselves to a description of axially symmetric solutions. This approximation is important for many practical cases, because under axial symmetry of the resonator and active medium, beam quality proves to be highest. We shall concentrate our attention to the large class of tube gas discharge lasers of either diffusion cooled type or fast axial flow (FAF) conception. The basic mathematical model for these two cases is the same; it is presented below. The differences are connected with radial dependence of small signal gain (SSG). These two cases are considered separately in Section 3.

Following the procedure described in detail in [5] we use the analytical solution of the diffraction problem for a narrow ring slit. The diffraction field from an infinitely narrow ring of radius r_0, for linear polarization at the distance L, is expressed by the formula

$$\mathrm{DEL}(L,\theta,r_0) \approx 2\pi r_0 ik \frac{e^{ikL}}{L} e^{ik\frac{r_0^2}{2L}} J_0(kr_0\theta), \qquad (1)$$

where k is the wave vector, and J_0 is the zero-order cylinder Bessel function. The formula is valid at $L \gg r_0$. Reflection of an incident wave with a specified amplitude-phase distribution from a mirror is regarded as a Green-function problem. For an arbitrary amplitude-phase distribution of the initial field $E_0(r_0)$, the diffraction field at L distance (in vacuum) is calculated by performing the integration:

$$\begin{aligned} E(L,\theta) &\approx \int_0^{r_m} E_0(r_0)\mathrm{DEL}(L,\theta,r_0)\exp\left(-ik\frac{r_0^2}{R}\right)\mathrm{d}r_0 \\ &= 2\pi\frac{e^{ikL}}{L}\int_0^{r_m} r_0 E_0(r_0) \\ &\quad\times\exp\left[ik\left(\frac{r_0^2}{2L}-\frac{r_0^2}{R}\right)\right]J_0(kr_0\theta)\mathrm{d}r_0. \end{aligned} \qquad (2)$$

This formula is written for the first iteration step, when the initial field $E_0(r_0)$ is specified on a plane at the first mirror location, and the diffraction field is calculated on a spherical surface of L radius at the location of the other resonator mirror. This influences the form of the exponential multiplier in the integral. The phase emerges from the rings of different radii (r_0) at the distance L; it is also related to the mirror curvature R (positive for concave, negative for convex mirrors). The designation of the mirror radius is r_m.

All the consequent iteration steps except the first one use the incident field specified on the spherical surface of L radius, calculated at the previous step, and give results on a spherical surface too. In this case the exponential multiplier in the integrant has the following form: $\exp\left(ik\frac{r_0^2}{L}\left(1-\frac{L}{R_i}\right)\right)$, where $i = 1, 2$ is the index specifying the resonator mirror.

The paraxial approximation defines a large class of practically important open resonators. In these resonators the Fresnel number $F = \frac{r_m^2}{\lambda L}$ is evaluated in units. In Eq. (1) the phase term $\sim\frac{r_0^2}{\lambda L}$ and the argument of the Bessel function are of the same order. They vary from zero to Fresnel number F in the range of integration from zero to the mirror radius r_m.

The active medium in the resonator is modeled by the following well known formula for saturating gain:

$$\alpha(r) = \frac{\alpha_0(r)}{1 + I(r)/I_{\mathrm{sat}}(r)}, \qquad (3)$$

where $\alpha_0(r)$ is SSG, $I_{\mathrm{sat}}(r)$ is the saturation irradiance, and $I(r)$ is the field intensity, recalculated at every bounce. In the present model the properties of the active medium $\alpha_0(r)$ and $I_{\mathrm{sat}}(r)$ are homogeneous along the resonator axis. In any axially symmetric active medium there will be a certain radial dependence of α_0 and I_{sat}. There are at least two qualitatively different situations from the viewpoint of transverse mode formation. Taking into account gas discharge lasers we should consider at least two cases:

(a) Low power lasers, where the active medium can be modeled by a "bell shaped" gain radial distribution with the maximum value on axis.

(b) High-power lasers where some overheating at the axis (or other physical processes) strongly influences the radial distribution $\alpha_0(r)$. Typically it is the appearance of a gain dip on the axis. The distribution of saturation irradiance I_{sat} can be varied with changes of discharge current too.

Having an active medium and investigating the process of transverse mode formation from zero level up to the stationary state we should also include spontaneous noise into our integral. The integral with radiation amplification in the active medium is presented by the formula:

$$\begin{aligned} E_2^n(L,\theta) &= 2\pi\frac{e^{ikL}}{L}\int_0^{r_m} r_0 \exp\left(ik\frac{r_0^2}{L}\left(1-\frac{L}{R_1}\right)\right) \\ &\quad\cdot\exp\left[\frac{\alpha_0(r)\cdot L}{1+[E_1^{n-1}(r_0)/E_{\mathrm{sat}}(r)]^2}\right] \\ &\quad\times(E_1^{n-1}(r_0)+E_{\mathrm{sn}}(r_0))\cdot k_m\cdot J_0(kr_0\theta)\cdot\mathrm{d}r_0. \end{aligned} \qquad (4)$$

This formula shows the following:

- The amplitude-phase distribution of the field $E_1^{n-1}(r_0)$, computed at the previous step of calculations is taken as the incident radiation on the first mirror. Amplitude-phase distribution of $E_1^{n-1}(r_0)$ has come from the second mirror and is given on the sphere of L radius. This sphere center coincides with the center of the second mirror.
- The field $E_1^{n-1}(r_0)$ is reflected from the first mirror. This leads both to a phase change due to curvature radius R_1, and to an amplitude reduction due to the partially reflecting first (coupler) mirror with amplitude reflection coefficient k_m.
- The radiation then passes through an active medium presented by saturated gain (in square brackets). $E_{\text{sat}}(r)$ is the saturation irradiance field amplitude.
- The calculations start from the "spontaneous noise," $E_{\text{sn}}(r_0)$. Its radial dependence follows from the radial profile of the SSG but does not play an important role for the final results. The value of $E_{\text{sn}}(r_0)$ is negligible in comparison with $E_1^{n-1}(r_0)$, as soon as the generation has developed.
- The integral describes the diffraction field $E_2^n(L,\theta)$, the incident radiation on the second mirror, for the next step of calculations. Amplitude-phase distribution of $E_2^n(L,\theta)$ is given on the sphere of L radius; its center coincides with the center of the first mirror.

One cycle of calculations has two steps. They have some natural features.

$$E_1^{n-1} \Rightarrow E_2^n[E_1^{n-1}, R_1, k_m] \Rightarrow E_1^n[E_2^n, R_2] \Rightarrow E_1^n.$$

Let us take the field E_1^{n-1} incident to the first mirror (curvature R_1, reflectivity k_m). Thanks to reflection, diffraction, and gain in active medium, the field E_2^n can be calculated using Eq. (4). Then E_2^n is used as the incident field on the second mirror (curvature R_2, reflectivity is 100%). The field E_1^n is calculated using Eq. (4) with corresponding changes. Now we can start the next cycle of calculations using E_1^n instead of E_1^{n-1}.

In all consequent calculations the length of active medium is chosen the same as the resonator length. The Eqs. (2) and (4) can describe only axially symmetric modes like TEM_{p0} in terms of Laguerre Gaussian (LG) modes TEM_{pq} where p is radial and q is azimuthal indices.

The resonator simulation based on Eq. (4) has some advantages. The calculations do not require any substantial computational resources and heavy time expense. This allows the comparative research of the dynamics of mode formation to be carried out over a wide range of parameters. The program for simulation of a resonator based on the integral (4) was written in MathCad. The integral was calculated as series with 360 terms on the mirror radius of reflected mirror. Diffraction field on the next mirror was calculated with 360 steps also on its radius. Results are presented in the form of array of complex numbers (amplitude-phase field distribution) for both mirrors, chosen number of bounces with radial resolution of 360 steps. Typical computation time of 1000 bounces on a personal computer was about 15 minutes.

The method can be useful in investigating stable and unstable resonators with spherical, cone [7,8], and toroidal mirrors [9] by implementing the correct amplitude-phase factors for transition from the mirror surface to the calculation sphere of radius L at the same position. It can also be applied for radiation with radial (or azimuthal) polarization by changing the Bessel function appropriately [5].

Transverse mode formation in different types of lasers shows both common properties and type-specific features. If the laser parameters (the radius, the length of an active medium, and mirror curvature radii) are chosen in such a way that only the principal mode has small losses, the final result is quite predictable. A single principal mode will generate independently of pumping conditions. From the viewpoint of the principal mode formation there are some optimal resonator parameters $(\text{L}, r_m, R_1, R_2)$ giving a competitive advantage to the principal mode. If, for example, the value of r_m is reduced (in comparison with the optimal situation), the losses of the principal transverse main mode will be increased at each bounce and the laser efficiency will go down. At large r_m other modes can compete with the principal one. The laser goes out of the regime of principal mode generation. This quite natural behavior is also observed in our numerical experiments.

If the conditions exist for generation of higher order modes, we can observe some specific features of the transverse mode formation because the active medium plays an important role in this process. The researchers and producers of lasers very often want to obtain a high quality laser beam, but in many cases it is difficult or even impossible to satisfy the conditions of principal mode generation. There are many examples of such kind related to wide aperture lasers: high-power industrial lasers, disk solid state lasers, VECSEL, extremely high-power lasers for thermo nuclear investigations, or military applications. Even if we restrict ourselves to gas discharge tube lasers there are two qualitatively different situations.

The first group includes the lasers in which the generation of an individual non-principal LG mode is impossible. In this group there are lasers of low power (like He-Ne lasers) and high-power industrial CO_2 lasers with transverse high frequency pumping. For example high quality He-Ne lasers are offered on the market either as fundamental mode or "multimode," the latter having an uncertain field structure over the beam cross-section.

The second group includes the lasers that are able to generate a single non-principal LG mode. The typical representatives of this family are FAF CO_2 lasers with longitudinal direct current (DC) discharge pumping. One of them will be discussed later.

It seems natural to assume that the qualitative features of transverse mode formation for these two groups can be explained by the qualitative difference of gain radial distribution. In the first case we have gain radial distribution with maximum amplification at the axis. In the second one there is some (small or big) gain dip at the tube axis. We shall consider these cases separately.

A. Lasers with On-Axis Gain Maximum

Low power lasers are usually diffusion cooled and pumped by longitudinal DC discharge in a glass tube. In this case the radial dependence of α_0 can be correctly modeled by a zero-order Bessel function $J_0\left(2.405\frac{r}{r_m}\right)$. Indeed, according to Schottky theory [10,11] we have this function for the distribution of electron density, so the use of the same radial function for α_0 is physically justified. The saturation irradiance I_{sat} is taken constant for simplicity in this part.

Figure 1 illustrates what happens to the magnitude of the electric field if the mirror radius is increased while retaining the absolute value of SSG and its radial form J_0. This corresponds to low power lasers without overheating at the axis. One can see that increasing the tube radius increases the number of bounces required to reach steady state. The time of the principal mode establishment corresponds to several bounces for $r_m \cdot k = 5000$ and increases up to about 750 bounces for $r_m \cdot k = 6640$. Finally, in Fig. 2 we obtain a quasi-stationary situation of "multimode generation" at $r_m \cdot k = 6650$ and larger. Figure 2 illustrates two different situations. In Fig. 2a one can see the regular oscillations with a period of three bounces. It is because the chosen resonator parameters correspond to the conditions of three-pass paraxial resonance at $g_1 = g_2 = 0.5$ [5,6]:

$$g_1 \cdot g_2 = \frac{1+\cos\theta}{2}; \qquad \theta = 2\pi\frac{K}{N}; \qquad 0 \le K \le N/2, \tag{5}$$

where N is the number of resonator round-trips required to form a closed ray trajectory. $g_i = 1 - \frac{L}{R_i}$ are the parameters of the stability diagram of open resonators, $i = 1, 2$. So we obtain here the "multi pass ray mode" described in [6]. In Fig. 2b the resonator parameters are out of paraxial resonance. One can see irregular oscillations of quasi-stationary generation.

B. Lasers with Off-Axis Gain Maximum

In high-power lasers, diffusion cooled, or FAF CO_2 lasers, the situation is more complicated. The radial function of α_0 depends on a number of factors: the form of discharge (DC longitudinal or HF transverse), the principle of gas cooling (diffusion or convection), and the type of gas flow (laminar or turbulent). In diffusion cooled lasers one can observe overheating of the active medium at the tube axis with a remarkable gain decline there. In FAF CO_2 lasers with DC pumping there is only a small gain reduction at the axis, explained by a number of competing physical processes. In both cases we deal with a specific qualitative feature: a gain decrease at the tube center. When studying these very cases we decided to base ourselves on the experimental measurements of active medium obtained in [12,13] for FAF CO_2 laser amplifier. The turbulent gas flow (it was up to 180 m/s in [12,13]) smooths the gain radial distribution but nevertheless at high pumping there is a small reduction of gain at the tube axis too. The radial distribution of SSG was modeled as a subtraction of two parabolas of fourth and second orders. The functional dependence of relative portions of these parabolas was unified for all the curves in Fig. 3 and chosen to model the experimentally obtained results [12,13] in the best way. One can see the shift of maximum gain from the tube center (at low discharge current) in the direction of the wall as the current is increased.

Figures. 4–6 show the main features of transverse mode formation while the field is developing in the laser. All these curves except for that in Fig. 6b differ from each other only by SSG (its value and radial distribution, see Fig. 3), all other parameters being the same. The relative size of main mode caustic on the mirror $w_1/r_m = w_2/r_m = 0.242$ is small. Multimode generation is possible, but at comparatively low gain (close to the threshold of generation) the principal mode generation is obtained.

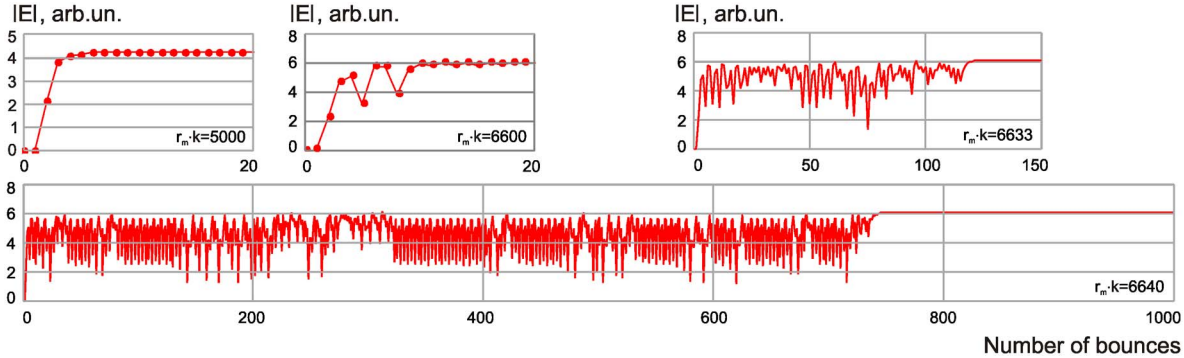

Fig. 1. (Color online) Evolution of the field amplitude at the mirror center in the laser for different mirror radii. Parameters: $L \cdot k = 2,543,000$, $R_1 = R_2 = 2L$. SSG is presented by the formula $\alpha_0 \cdot L = 5.4 \cdot J_0\left(2.405\frac{r}{r_m}\right)$.

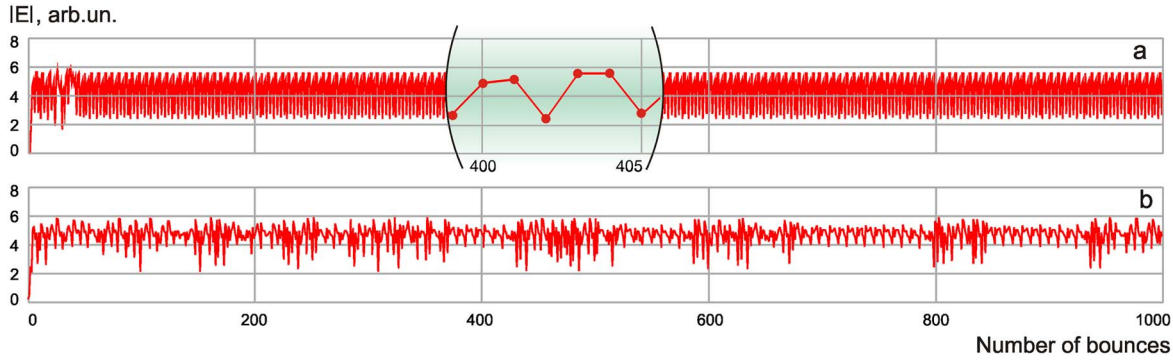

Fig. 2. (Color online) Evolution of the field amplitude at the mirror center in the laser at "multimode" quasi-stationary generation. Parameters: $r_m k = 6650$, $L \cdot k = 2,543,000$. SSG is described by the following formula: $\alpha_0 \cdot L = 5.4 \cdot J_0(2.405\frac{r}{r_m})$. The upper picture (a) is for $L/R_1 = L/R_2 = 0.5$, three-pass paraxial resonance conditions. In the center of (a) an enlarged section of field oscillations is shown. The lower figure (b) is for $L/R_1 = L/R_2 = 0.45$. The conditions are out of paraxial resonance.

Figure 4 illustrates in particular that increasing SSG results in less time to reach steady state, principal mode. Figure 5 shows how the mode TEM_{10} is formed. One can see a very interesting feature here. For some time (shorter than 50 bounces on the abscissa scale) stable generation is obtained with the radial distribution close to the principal mode. Then this state becomes unstable and TEM_{10} is formed after relaxation oscillations. For higher pumping the stair becomes shorter, see Fig. 6. It illustrates different types of relaxation oscillations for paraxial resonance conditions and out of paraxial resonance. To further illustrate the physical reality of the model we have performed a numerical Rigrod analysis (output power as a function of output coupler reflectivity). Calculated results fit the theoretical Rigrod curve well as illustrated by Fig. 7. The output power was calculated as an integral of squared field amplitude over the radius.

3. Experimental Example

The experimental setup is a square-folded, DC-excited, fast-axial-flow 4 kW CO_2 laser. The details of its design and the construction principle can be found in [15]. The main features of importance here are: 22 mm aperture, 4290 mm resonator length, and about 300 m/s average gas velocity. The latter is provided by a high-speed, three-stage compressor producing a mass flow of 1 m^3/s of a $He{:}N_2{:}CO_2 = 85{:}13{:}2$ mixture at 13,000 Pa, divided over eight 300 mm long discharges. The resonator is symmetric with 20 m concave mirrors, one of which has a power transmission coefficient of 40%. It should be noted that for all levels of output power of practical interest (>500 W), a single higher order "bull's eye" mode is obtained. The single-mode character is further demonstrated by the invariance of the beam profile with distance, at least up to a distance of 20 m from the laser output coupler. Qualitatively, the following steady state transverse modes can be observed: at extremely low output power (<100 W) a small dot, too weak to establish its nature by scanning with a rotating needle beam analyzer (which was configured for kW level power). In the region between 100 and 500 W, a ring shaped mode profile with a central dip is observed. At all the power levels of practical interest a clear "bull's eye" mode profile is seen: a bright central hot spot surrounded by a slightly less intense outer ring. The dark space between the central hot spot and the outer ring is very pronounced and alignment sensitive. In fact it is used in practice as an indicator of correct alignment. Figure 8 shows the experimentally obtained laser modes: the ring shaped mode profile and the "bull's eye" mode at low

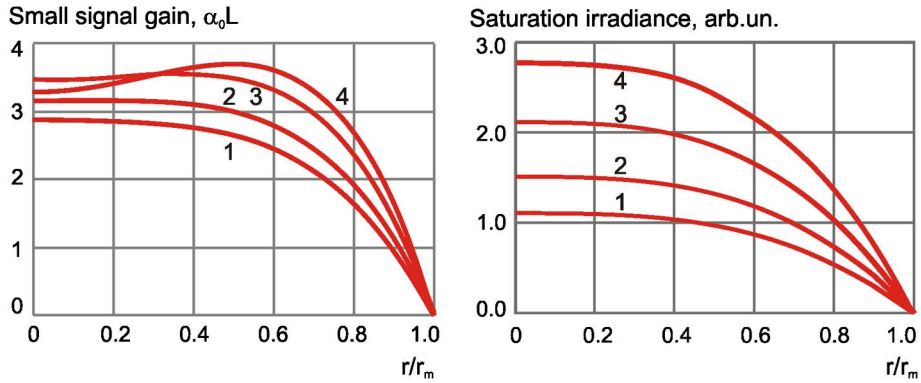

Fig. 3. (Color online) Radial distribution of SSG (left) and saturation irradiance (right). Curves 1, 2, 3, 4 correspond to $\alpha_0 L = 2.88$, 3.08, 3.38, 3.7 at the axis, respectively.

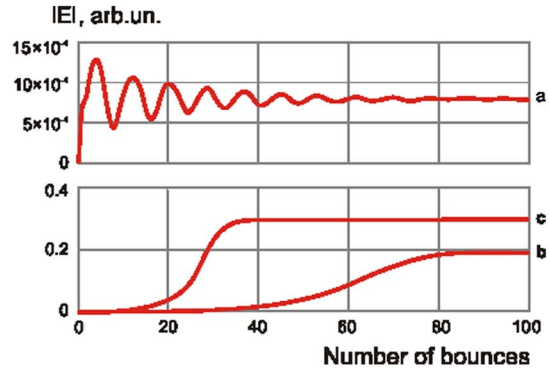

Fig. 4. (Color online) Evolution of the field amplitude at the mirror center in a symmetric resonator at low SSG. Parameters: $r_m k = 10,000, L = 254 r_m, R_1 = R_2 = 2L$. The curves are for different values of SSG: (a) $\alpha_0 L = 2.88$ (below the threshold of generation); (b) and (c) $\alpha_0 L = 2.94$ and 3.00, correspondingly (above the threshold of generation).

(a) and high (b) gain. Measurements were made with rotating hollow needle beam analyzer "primes." Measurements were made at 210 mm from the output coupler in both cases and the outer circle displayed shows the 22 mm resonator aperture to scale. The small circle is located at the radius of zero field. Because of the rather coarse nature of the scanning device (only 128×128 pixels scanning a 60×60 mm square cross section) some kind of averaging was necessary to reduce the spiky appearance of the data. The pictures obtained are the average of four measurements.

The results presented in Fig. 8 were obtained for the resonator parameters of the experimental laser. The chosen radial distribution of gain and saturation irradiance is given in Fig. 3; they are close to experimentally measured profiles [13]. The gain has some small reduction on the tube axis at high pumping. The exact parameters of our device differ from the laser studied in [12,13], regarding gas velocity and the gain profile. Nevertheless, the behavior of the central dip should be similar to that of the dip in Fig. 3. It becomes even more pronounced at higher speed [12], but the flow profile itself becomes flatter near the axis.

The ring type mode obtained experimentally, Fig. 8a, cannot be calculated by using the theoretical model developed in Section 2 in spite of its apparent "axial symmetry." Experimentally obtained, such a field distribution (doughnut mode) has a specific nature. Two possible explanations of this phenomenon are known. First it can be the time averaged noncoherent superposition of TEM_{01} modes chaotically jumping around the axis. This assumption looks quite natural because the TEM_{01} mode is inhomogeneous along the azimuth but pumping typically has an axial symmetry. Another possibility is the helical mode; it is realized in the form of two spots of the TEM_{01} mode, uniformly rotating around the axis over any cross section of the beam. In any of these two cases momentary radial distribution of the field corresponds to the pure TEM_{01} mode. This mode is not axially symmetric; therefore it is out of the boundaries of applicability of the presented numerical model.

The calculations, Fig. 9, illustrate the generation of a TEM_{10} mode called the "bull's eye" mode in the experiments. The calculations and experiment are in excellent agreement, keeping in mind the location of the zero field zone between the peak and the ring. The calculated phase radial distribution is close to the idealized LG mode TEM_{10}. In particular it gives a good chance to improve the focusing properties of such a beam using phase correction that provides a local π-phase drop in the peak (or ring) of TEM_{10} mode. This results in the same phase over the beam cross section.

Similar experiments were performed by the authors with lasers of the same basic design but different resonator configurations. These experiments always reveal the same sequence of mode generation as a function of gain level: principal mode, one ring doughnut mode, peak plus ring mode (TEM_{10}), double ring doughnut mode, and peak plus two rings

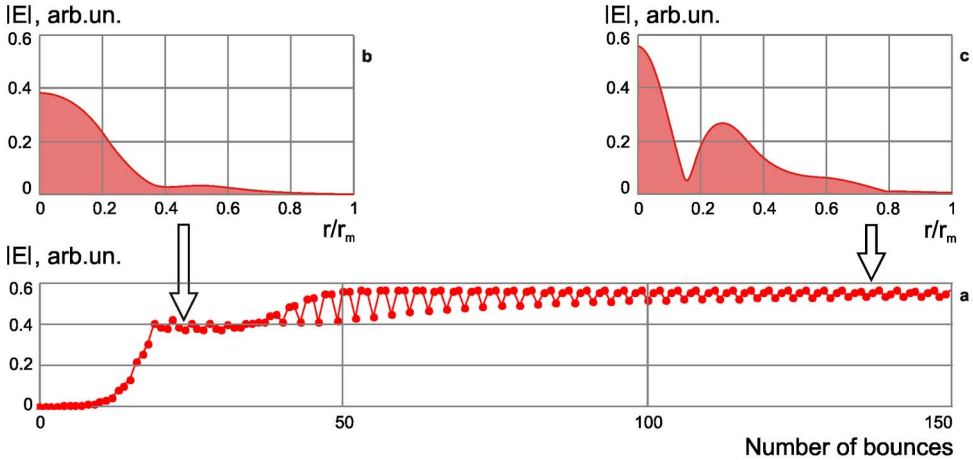

Fig. 5. (Color online) Evolution of the field amplitude at the mirror center in a symmetric resonator at SSG $\alpha_0 L(r/r_m = 0) = 3.08$. All other parameters are the same as in Fig. 4.

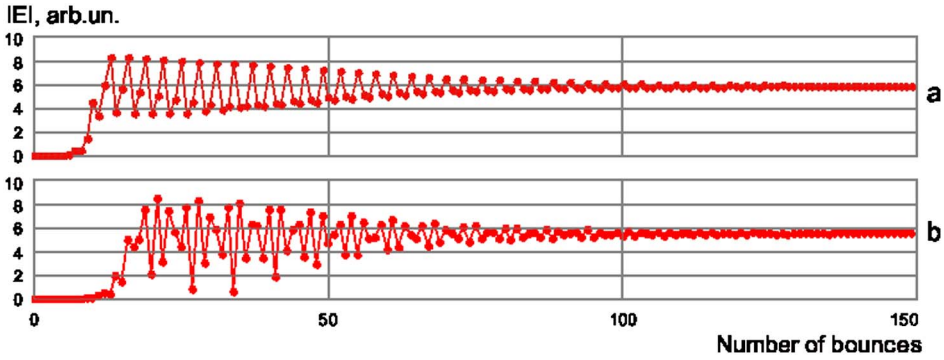

Fig. 6. (Color online) Evolution of the field amplitude at the mirror center in a symmetric resonator at SSG $\alpha_0 L(r/r_m = 0) = 3.38$ for both the curves. (a) All other parameters are the same as in Fig. 5. They correspond to the conditions of paraxial resonance. (b) Parameters of calculations: $r_m k = 11,860$, $L = 214 r_m$, $R_1 = R_2 = 4.66L$ are out of the conditions of paraxial resonance.

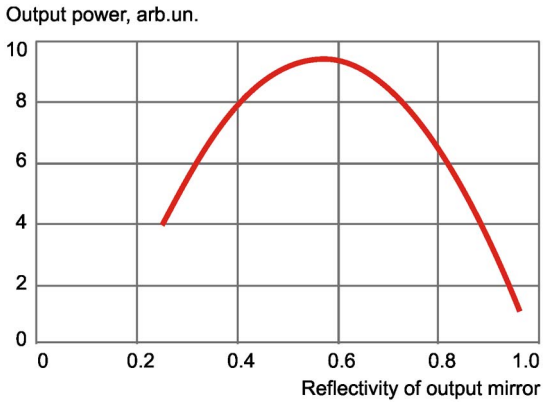

Fig. 7. (Color online) Dependence of output power on reflectivity of the couple mirror (Rigrod's formula [14]) as a result of numerical experiment. Parameters: $r_m k = 10,000$, $L = 254 r_m$, $R_1 = R_2 = 2L$. SSG $\alpha_0 L(r/r_m = 0) = 3.08$. Radial dependence of gain is presented in Fig. 3, curve 2.

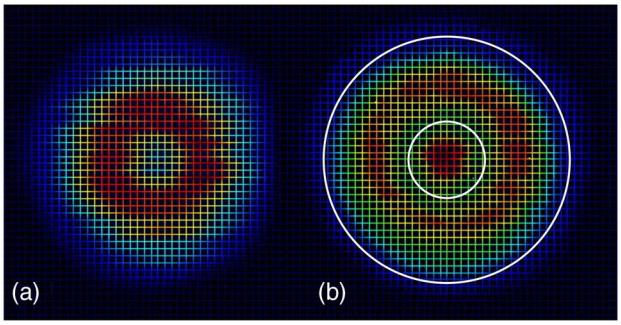

Fig. 8. (Color online) Doughnut mode (a) and TEM_{10} mode (b) obtained experimentally. The small circle is located at the radius of minimum intensity of laser beam between peak and ring. The red color corresponds to maximum radiation intensity. The big circle shows the aperture size.

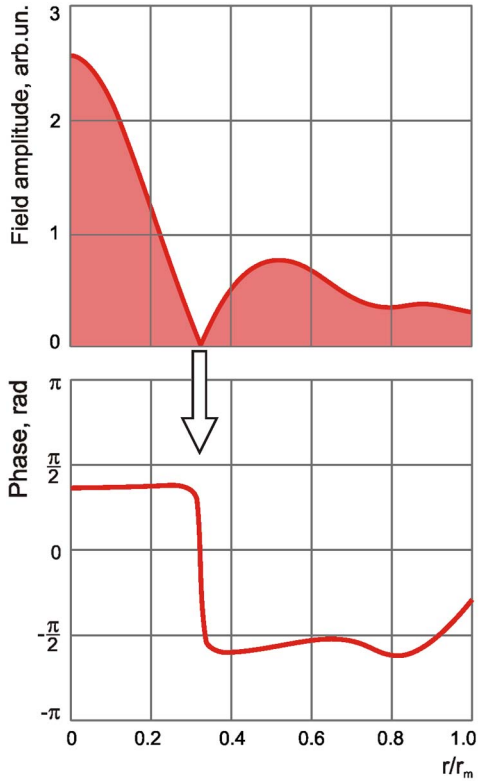

Fig. 9. (Color online) Radial dependences of the established field amplitude (up) and phase on the mirror (down). Parameters: $r_m k = 6517$, $L = 390 r_m$, $R_1 = R_2 = 4.66 \cdot L$. SSG $\alpha_0 L(r/r_m = 0) = 3.4$. Radial dependences of gain and saturation irradiance are presented in Fig. 3. The arrow points to the location of the phase drop.

mode (TEM_{20}) and so on until a limit determined by the Fresnel number.

In higher order modes for the bigger aperture the calculated phase radial distribution is not as perfect as it was for the TEM_{10} mode, see Fig. 10. If a higher order mode can be obtained experimentally in the form of a peak and rings of radiation intensity, it does not mean that the phase of this mode can be effectively unified by a simple stepped (0–π–0) phase corrector. The phase distribution of a real mode is rather smoothed in comparison with the idealized LG mode TEM_{20}.

The competitive possibility of a concrete mode depends on two opposite effects: the mode feeding from the active medium into the mode volume and the mode losses on the mirror edges. The radius of location of gain maximum is increased as pumping is risen. It gives a competitive advantage for the higher order mode. This advantage is effectively realized if the aperture is large enough. It is a very interesting

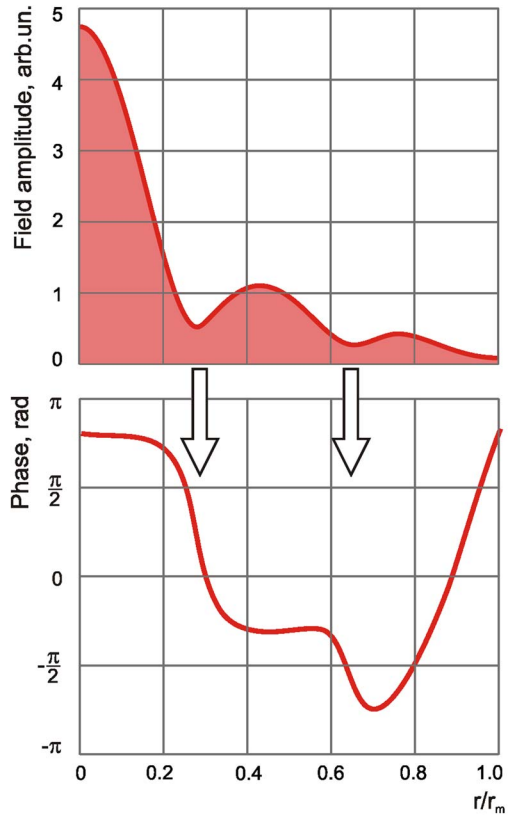

Fig. 10. (Color online) Radial dependences of the established field amplitude (up) and phase on the mirror (down). Parameters: $r_m k = 7500$, $L = 339 r_m$, $R_1 = R_2 = 4.66 \cdot L$. SSG $\alpha_0 L(r/r_m = 0) = 3.7$. The radial dependences of gain and saturation irradiance are presented in Fig. 3. The arrows point to the location of the phase drop.

result that a high-power laser (FAF DC pumping CO_2 laser) can have better transverse mode structure than a low power laser (He-Ne laser). It can be observed for a Fresnel number more than one, and it is explained by different structure of the active medium.

Lastly, we compare the results of our calculations with the experiments in [6]. Unfortunately the detailed description of the experimental setup is absent there. The natural suggestion is that in 1970 they used an "old fashioned" tube diffusion cooled low power DC excited CO_2 laser. It has an on-axis gain maximum and in the "multimode regime" we obtain quasi-stationary generation which gets transformed into a multipass ray mode at the conditions of paraxial resonance. So we have good agreement of our calculations and those experiments. Another result obtained in [6] is not confirmed by our calculations. It is the existence of dips on the experimental dependence of measured output power as a function of mirror separation. These dips occur at the paraxial resonance positions. In our calculations there are no such dips. The possible reason of this contradiction is a different way of extraction of output power from the laser. In our case it is a semitransparent output mirror. The authors of [6] detected the output power through the hole of 0.1–1 mm diameter made in the mirror. These conditions are too different to be compared.

4. Conclusion

A numerical model for simulation of an axially symmetrical resonator with an active medium is developed. The model is based on an analytical formula of radiation diffraction from a narrow ring. Reflection of an incident wave with a specified amplitude-phase distribution from the mirror is regarded as a Green-function problem. It also includes an active medium homogeneous along the resonator axis and is simulated by the formula for saturated gain.

The calculated results are presented for two types of lasers: with on-axis gain maximum and with off-axis gain maximum. In spite of the fact that the gain dip is very small in the second case, the transverse mode formation is qualitatively different in these two cases.

In the first case (typical for low power diffusion cooled tube lasers) we can obtain either principal mode generation or "multimode" beam. The last one is shown to be quasi-stationary generation. It is realized in the form of multi pass ray mode if the resonator parameters correspond to the conditions of paraxial resonance. If the resonator parameters are out of paraxial resonance irregular field oscillations are observed.

In the second case (typical, for example, for a FAF CO_2 laser), the single modes of different order starting from the principal one can be obtained consequently at the increasing current. Oscillations leading to mode formation can be regular for paraxial resonance conditions or irregular when the resonator parameters are out of paraxial resonance.

The calculated results are in good agreement with the experimental investigations performed on the FAF 4 kW CO_2 laser. The calculated phase radial distribution is close to the idealized LG mode TEM_{10}. The calculated phase distribution of the real mode having a peak and two rings is rather smoothed in comparison with the idealized LG mode TEM_{20}.

The authors thank Yu. N. Zavalov for useful discussions.

References

1. A. E. Siegman, *Lasers* (University Science Books, 1986).
2. N. Hodgson and H. Weber, *Optical Resonators: Fundamentals, Advanced Concepts and Applications* (Springer Verlag, 1997).
3. Y. A. Anan'ev, *Laser Resonators and the Beam Divergence Problem* (Institute of Physics, 1992).
4. H. A. Haus, *Waves and Fields in Optoelectronics* (Prentice-Hall, 1984).
5. V. G. Niziev and R. V. Grishaev, "Dynamics of mode formation in an open resonator," Appl. Opt. **49**, 6582–6590 (2010).
6. I. A. Ramsay and J. J. Degnan, "A ray analysis of optical resonators formed by two spherical mirrors," Appl. Opt. **9**, 385–398 (1970).
7. Anatol N. Khilo, Eugeny G. Katranji, and Anatol A. Ryzhevich, "Axicon-based Bessel resonator: analytical description and experiment," J. Opt. Soc. Am. A **18**, 1986–1992 (2001).

8. E. F. Yelden, H. J. J. Seguin, C. E. Capjack, S. K. Nikumb, and H. Reshef, "Toric unstable CO_2 laser resonator: an experimental study," Appl. Opt. **31**, 1965–1974 (1992).
9. Masamori Endo, "Azimuthally polarized 1 kW CO_2 laser with a triple-axicon retroreflector optical resonator," Opt. Lett. **33**, 1771–1773 (2008).
10. Y. P. Raizer, *Gas Discharge Physics* (Springer Verlag, 1997).
11. W. Schottky and J. Issendoff, "Über die Whärmewirkung kathodischer Gehäuseströme in Quecksilberentladungen," Z. Phys. A Hadrons Nuclei **26**, 85–94 (1924).
12. N. Takahashi, E. Tsuchida, and H. Sato, "Spatial variation of gain and saturation in a fast axial flow CO_2 laser amplifier," Appl. Opt. **28**, 3725–3736 (1989).
13. E. Tsuchida and H. Sato, "Dependence of spatial gain distribution on gas-flow velocity and discharge current in a FAF CO_2 laser amplifier," Jpn. J. Appl. Phys. **28**, 396–405 (1989).
14. W. W. Rigrod, "Saturation effects in high-gain laser," J. Appl. Phys. **36**, 2487–2490 (1965).
15. D. Toebaert, "An integrated approach to laser machine tool fabrication," Laser User **49**, 30–31 (2007).